Radial Hermite Operators for Scattered Point Cloud Data with Normal Vectors and Applications to Implicitizing Polygon Mesh Surfaces for Generalized CSG Operations and Smoothing

Gregory M. Nielson

Arizona State University

ABSTRACT

We describe a new technique for fitting scattered point cloud data. Given a scattered point cloud of 3D data points and associated normal vectors, our new method produces an implicit volume model whose zero level isosurface interpolates the given points and associated normal vectors. In this paper, we concentrate on certain application of these new volume modeling techniques. We take existing polygon mesh surfaces and use the present methods to construct implicit volume models for these surfaces. Implicit models allow for the application of Boolean operations on these surfaces through the techniques of constructive solid geometry. Also, standard wavelet and filter operators can be applied to the implicit volume model leading to effective smoothing and filtering algorithms which are simple to implement.

CR Categories: I.3.5 [Computer Graphics]: Computer Graphics – Computation Geometry and Object Modeling – surface, solid and object representations

Additional Keywords: Surface reconstruction, point clouds, isosurfaces, polygon mesh

1 INTRODUCTION

In this paper, we describe a new technique for constructing an implicit, 3D volume model from points with associated normal vectors. Given a scattered point cloud,

$$P_i = (x_i, y_i, z_i), i = 1, \cdots, M$$

and associated normal vectors

$$N_i = (Nx_i, Ny_i, Nz_i), i = 1, \cdots, M$$

we describe an implicit model $\rho(x, y, z)$ such that

$$\rho(P_i) = \rho(x_i, y_i, z_i) = 0, i = 1, \cdots, M$$

and

$$\nabla\rho(P_i) = \left(\frac{\partial\rho}{\partial x}(P_i), \frac{\partial\rho}{\partial y}(P_i), \frac{\partial\rho}{\partial z}(P_i)\right) = N_i, i = 1, \cdots, M$$

nielson@asu.edu

IEEE Visualization 2004
October 10-15, Austin, Texas, USA
0-7803-8788-0/04/$20.00 ©2004 IEEE

The interpolation conditions above imply that the isosurface

$$S = \{(x, y, z): \rho(x, y, z) = 0\}$$

passes through the points P_i, $i = 1, \cdots M$ with the associated normal vectors, N_i at these points.

Our new method draws upon the ideas and previously established successful methods from scattered data modeling (see Nielson [18]). While there are fundamental similarities, we should point out that the problem of point cloud fitting should be distinguished from that of scattered data modeling (see Franke and Nielson [13]). While it is true that many of the basic techniques and tools from CAGD and multivariate approximation theory apply to both, the two problems are basically different. One fundamental connection between them is through some type of parameterization of the point cloud, (see Floater [9]), whether this be implicit or explicit, but this relationship is not well and completely understood today. The phrase "scattered data fitting" was coined by Schumaker in his 1976 paper [26] and there was a great deal of interest and published research on (mainly) bivariate problems in the 70s and 80s. With the advent of scientific visualization along with volume visualization in the 90s, there was growing interest in trivariate scattered data modeling (see Nielson [18], Nielson [19], Nielson [20], Nielson & Tvedt [22] and Bertram [4]) and interest in this area continues to grow. In many respects, the problem of scattered point cloud fitting is more difficult because it is less understood, but the widespread and strong need for practical and effective methods for point cloud fitting make this an important problem. Today, there is widespread interest in the problem and many algorithms, methods and techniques are being proposed. See Müller [17] for a survey on the topic and for a sampling of specific methods consult Zhao et al [34] , Xie et al [33], Algorri et al. [1] and Bernardini et al. [3].

A number of methods involve the signed distance function, $D(P)$, which is a trivariate function with the convention that it is negative interior to S and positive outside of S. The surface is extracted from $D(P)$ as a triangular mesh surface approximation to the zero level isosurface. Typically, $D(P)$ is sampled on a 3D rectilinear grid and a method like the marching cubes algorithm (see Nielson [21]) is used. Once it is decided what the metric or the definition of distance from a surface to a point cloud is to be, it is usually not too difficult to develop algorithms for the efficient computation of the distance function. (See Sigg et al [29] for methods utilizing graphics hardware.) The particular difficulty here is getting the sign right; that is, to be able to efficiently and effectively determine when a point is inside the surface or outside. Typical of the methods based upon distance functions is that of Hoppe et al. [14] where the sign is based upon local least squares estimates of the normal vector of the surface and a consistent

orientation (in or out) is sought with the Riemannian map estimate. One of the drawbacks to this method is the heuristics of the signed distance function calculation may lead to gaps in the surface and the difficulty of choosing the proper resolution for the marching cubes voxel grid can have detrimental effects on the success of the method.

The new, adaptive, least squares method of Nielson et al. [25] is rather different from the present method. Starting with an initial approximation, the triangular mesh surface is refined in a region of largest error and a constrained least squares criterion is used to obtain a new optimal fitting surface. Two aspects of this method are particularly attractive. The adaptive aspects allow the efficient operation of the complexity of the triangular mesh approximation to conform to the complexity of the point cloud. The least squares aspect allows the method to be applied to noisy, non-uniform data sets. One of the present drawbacks to this method is that the initial approximation must have the same genus as the final optimal fitting surface.

Another important concept involved in point cloud fitting problems is the Delaunay tetrahedrization (see Nielson [19]) and its dual, the Dirichlet tessellation and Voronoi diagram. The method based upon alpha shapes of Edelsbrunner and Mucke [8] is a typical and early example. Here the first step is the Delaunay tetrahedrization. The second step is to apply the alpha-erasure to remove tetrahedra, triangles and edges whose minimum surrounding sphere is not contained in the alpha–erasure sphere. The result is called the alpha-shape. In the third step, triangles for the final surface are selected so that a sphere of radius alpha containing the triangle does not contain any other point cloud points. The main negative aspect of this approach is the choice of a suitable value of alpha. Too big of a choice leads to poor approximations not utilizing many of the points of the point cloud and too small a choice leads to gaps and fragmented surfaces.

Our new technique is most closely related to the distance function methods in that the approximating triangular mesh surface is characterized as the zero level isosurface of a volume model (trivariate field function). (See also Hotz [13].) Contrary to the techniques of Turk and O'Brien [31], Carr et al. [6], Morse et al. [16], our new method does not require the solution of linear systems of equations. Also, rather than require additional interior and exterior points, our new method requires normal vectors. We have selected an application of our new method where it is easy to compute consistent and accurate estimates of normal vectors. This application is the implicitization of polygon mesh surfaces. It is well known that some of the very useful operations of CSG such as union, intersection and blends are really rather difficult to implement for objects defined as being bounded by polygon mesh surfaces. But these operations are relatively easy to implement for "solid" objects defined implicitly by volume models (field functions). We illustrate the power of these new techniques with examples where objects that are originally defined as polygon mesh surfaces can be intersected, unioned and blended into new polygon mesh surface very simply with easily implementable methods utilizing some off-the-shelf techniques. Section 2 consists of the basic description of our new method and several examples are given in Section 3 and Section 4.

2 Implicit Radial Hermite Models for Scattered Point Clouds with Normals

Many of the ideas for our radial Hermite implicit models originate from the basic ideas of inverse distance weighted interpolation. As background information, we now describe this particular type of scattered data interpolation scheme. Given the data $(P_i, f_i), i = 1, \cdots M$, where $P_i = (x_{1_i}, x_{2_i}, \cdots, x_{n_i})$ is a point location and f_i is a dependent scalar value, sampled at that point, the following function has the property that it matches or interpolates to this data

$$S(P) = \frac{\sum_{i=1}^{M} \frac{f_i}{\|P - P_i\|}}{\sum_{i=1}^{M} \frac{1}{\|P - P_i\|}}. \quad (1)$$

That is,

$$S(P_i) = f_i, i = 1, \cdots, M . \quad (2)$$

The basic interpolation properties are easily verified if we write the interpolant of (1) in the following alternate form

$$S(P) = \sum_{i=1}^{M} w_i(P) f_i \quad (3)$$

where

$$w_i(P) = \frac{\prod_{j \neq i} \|P - P_j\|}{\sum_{i=1}^{M} \prod_{j \neq i} \|P - P_j\|}. \quad (4)$$

It is then easy to verify that

$$w_i(P_j) = \delta_{i,j} = \begin{cases} 1, i = j \\ 0, i \neq j \end{cases}$$

and so S has the interpolation properties as claimed in equation (2) above.

We now make two important changes. We move to implictly defined surfaces and restrict the data to be from 3D as this is the domain of the applications we have in mind. We use the notation $\langle P, Q \rangle = xu + yv + zw$ where $P = (x, y, z)$ and $Q = (u, v, w)$.

Theorem 1. (**Implicit, Hermite Inverse Distance Interpolant**) Let $P_i = (x_i, y_i, z_i)$; $N_i = (Nx_i, Ny_i, Nz_i), i = 1, \cdots, M$ be a point cloud with associated normal vectors and let S be the implicitly defined surface

$$S = \{P : \rho(P) = 0\}$$

where

$$\rho(P) = \frac{\sum_{i=1}^{M} \frac{\langle P - P_i, N_i \rangle}{\|P - P_i\|}}{\sum_{i=1}^{M} \frac{1}{\|P - P_i\|}} \quad (5)$$

then the surface S passes through the points P_i and has a normal vector at the point P_i equal to N_i.

Proof: As above, it is easier to analyze S if we rewrite ρ in the form

$$\rho(P) = \sum_{i=1}^{M} w_i(P) \langle P - P_i, N_i \rangle$$

where,

$$w_i(P) = \frac{\prod_{j \neq i} \|P - P_j\|}{\sum_{i=1}^{M} \prod_{j \neq i} \|P - P_j\|}.$$

In order to verify that P_i is actually on the surface, S, we need only note that $\rho(P_i)=0$. Since, in general, the normal vector at a point of an implicitly defined surface is the gradient of the field function at this point we need to compute the gradient of ρ at P_i. We use the product rule to obtain

$$\nabla\rho(P)=\begin{pmatrix}\frac{\partial\rho(P)}{\partial x}\\ \frac{\partial\rho(P)}{\partial y}\\ \frac{\partial\rho(P)}{\partial z}\end{pmatrix}=\sum_{i=1}^{M} w_i(P)\nabla\langle P-P_i,N_i\rangle+\langle P-P_i,N_i\rangle\nabla w_i(P)$$

Since $\nabla(P-P_i,N_i)=N_i$ and $w_j(P_i)=\delta_{i,j}$ we have that

$$\nabla\rho(P_i)=N_i, i=1,\cdots,M$$

and this completes the proof.

While the simplicity and elegance of the interpolants of (1) (and (5)) are appealing, it has been pointed out by several authors (see Franke and Nielson [10], [11] for example) that in actual applied practical problems, pure, inverse distance interpolants do not work very well. We will draw upon the success of previous modifications to (1) to obtain modifications of (5) which work well for the application domain we are covering here.

2.1 Radial, Hermite Interpolants

The overall general form of our implicit model will be

$$\rho(P)=\frac{\sum_{i=1}^{M}\frac{\langle P-P_i,N_i\rangle}{R_i(\|P-P_i\|)}}{\sum_{i=1}^{M}\frac{1}{R_i(\|P-P_i\|)}} \qquad (6)$$

where $R_i(x)$ is a univariate, C^1 function such that $R_i(0)=0, i=1,\cdots,M$. We call an implicit model of this type, a *radial Hermit* model or interpolant. The term *radial* connotes that the weight functions of the model are only functions of distance from an arbitrary point of the domain. The term *Hermite* conveys that the interpolant not only matches given dependent data values (zero in the present case) but also some type of first order variational quantity; which, in this case, are normal vectors which are the gradients (first derivative) of the field function.

As we mentioned earlier, $R_i(x)=x$ does not lead to very useful, practical methods of interpolating scattered data. One of the main drawbacks is the fact that the interpolant has C^1 discontinuities at the data sites. This can be alleviated with the use of $R_i(x)=x^{\mu_i}, 1<\mu_i$. The use of this radial function within the context of scattered data interpolants of the form of (1) above is call Shepard's method and has received considerable attention in the past. See Nielson [18], Nielson and Tvedt [22], Franke and Nielson [11]. Another significant drawback of (1) and also the Shepard's method is the extent of the influence of data points. Each point of the interpolant depends upon **all** of the data points. This, not only, can have adverse affects on the shape properties of the interpolant, but it also has negative impact on the computational aspects of any practical implementation of the method. In order to control the influence of data values, we borrow an idea from Franke and Nielson [10] (Modified Quadratic Shepard's, MQS) which limits the extent of the support of the weight functions $w_i(P)$. Combining this local support idea with variable exponents of the generalized Shepard's method we arrive at the following choice for the radial functions

$$\frac{1}{R_i(x)}=\left[\frac{(r_i-x)_+}{x}\right]^{\mu_i}, \text{ where } (z)_+=\begin{cases}z, z\ge 0\\ 0, z<0\end{cases} \qquad (7)$$

where the values r_i determine the radius of the disk of support for the weight functions.

3 Application to the Implicitization of Polygon Mesh Surfaces and Extended CSG Operations

In this section we show some applications of the implicit radial Hermite models of the previous section to triangular mesh surfaces. We will use these methods to produce a field function whose zero level isosurface is an approximation to a given triangular mesh surface. The points $P_i=(x_i,y_i,z_i), i=1,\cdots,M$ required for the radial Hermite model will be the vertices of a user provided polygon mesh surface. In addition to these vertices, the model of Equation (6) and (7) requires the associated normal vectors at each of the vertices. Computing estimates of normal vectors for polygon mesh surfaces is a common requirement as these values are often used in the rendering of surfaces. A survey and the comparison of a variety of methods can be found in Max [15].

Once the approximations of the normal vectors have been computed, the implicit model of equation (6) is defined. In order to render the implicitly defined surface, we compute a triangular mesh surface approximation using a marching cubes type of algorithm [21]. This requires samples of the field function (implicit model) on a rectilinear lattice grid. In Figure 1 we show an example. The input data for this example consists of a triangular mesh from www.cyberware.com. In this case there are 121,723 vertices. Normal vectors were computed with the simple averaging method and the implicit model was evaluated on a 180x120x300 grid. We used a uniform value for the exponents, $\mu_i=2$ and r_i was chosen so that the ball of radius r_i with center at P_i contains at least 18 data points. In order to illustrate the fact that the surface is the isosurface of a volume model, we have also included isosurfaces for negative and positive threshold values.

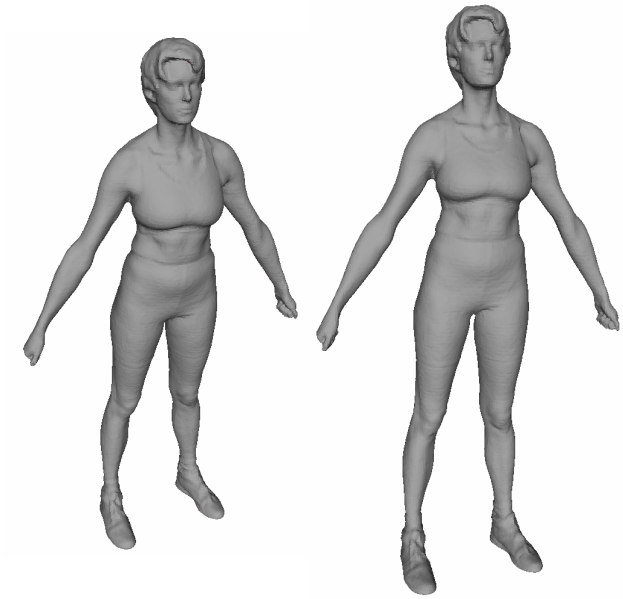

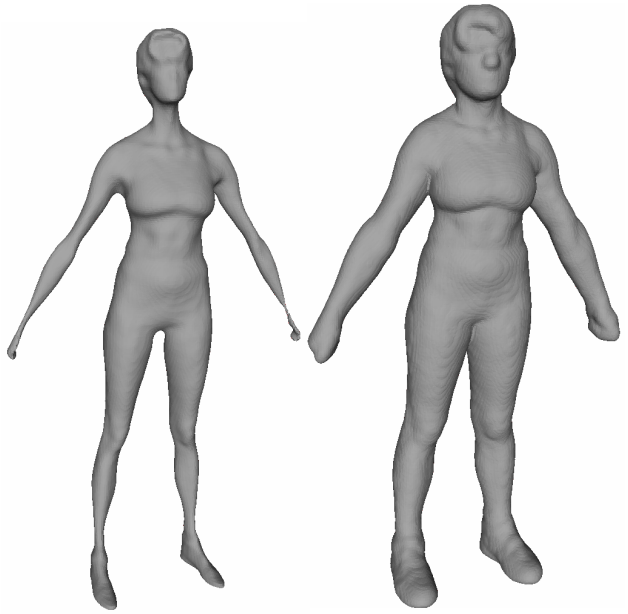

Figure 1. The upper left image is a triangular mesh surface from Cyber Ware with 121,723 vertices. The upper right is zero level isosurface extracted from a 180x120x300 sized sampling of the radial Hermite model using $\mu_i = 2$ and radii chosen so that each local ball contains at least 18 points. The lower left image is an isosurface with a negative threshold and the lower right image is an isosurface with a positive threshold value.

For this next example, we started with a fairly low resolution triangular mesh surface shown in the left image of Figure 2. We then applied Loop subdivision to refine and smooth the mesh as shown in the right image of Figure 2. In Figure 3, we show the isosurface of the implicit volume model. This illustrates another important feature of the volume model approach in that it is possible to sample the model at any desired resolution which leads to multiresolution model approximations of the surface.

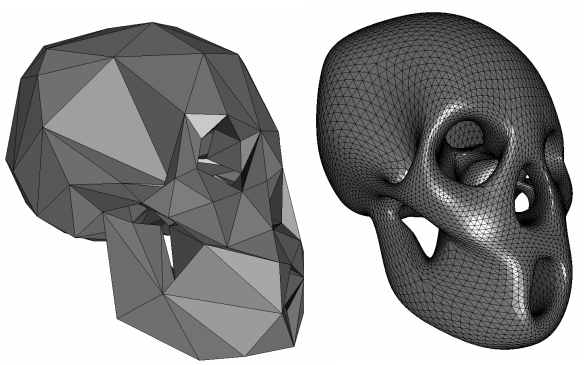

Figure 2. Triangular mesh surface and refined mesh using Loop subdivision.

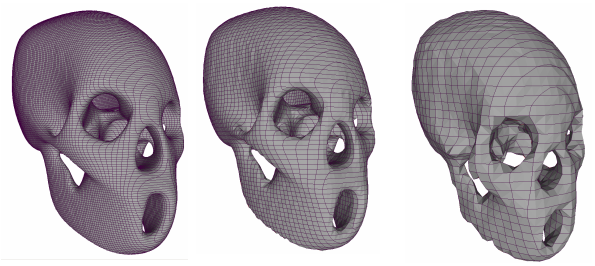

Figure 3. These images illustrate the possibility of obtaining multi-resolution models from implicit, radial Hermite models. In this case, the model is sampled at three resolutions and the zero level isosurface is extracted. The mesh on the left has 130,630 triangles, the middle mesh has 12,686 triangles and the right has 1,523 triangles.

We now discuss the Boolean operations associated with constructive solid geometry (CSG). Some notation will be useful in this regard. In general, we let F_A denote the volume model or field function for a point set A whose boundary is a surface of interest. That is

$$A = \{(x,y,z): F_A(x,y,z) \geq 0\} \tag{8}$$

For the present situation, F_A will be the radial Hermite model and the boundary of A is the implicitly defined approximation to a given polygon mesh surface as we described above. If B is another three dimensional point set with the volume model F_B, then it is easy to see that the *union* is defined by

$$A \cup B = \{(x,y,z): Max(F_A(x,y,z), F_B(x,y,z))\} \tag{9}$$

and so we have that

$$F_{A\cup B} = Max(F_A, F_B). \tag{10}$$

Similarly, we have for the *intersection*

$$F_{A\cap B} = Min(F_A, F_B) \tag{11}$$

and the *difference*

$$F_{A\cap \overline{B}} = Max(F_A, -F_B). \tag{12}$$

The *hyperbolic* blend is

$$F_{A\,\mathrm{HB}} = F_A F_B - 1$$

and the *super-elliptic* blend is

$$F_{A\,\mathrm{EB}} = 1 - \left\{Max(0,1-F_A)^{\beta} - Max(0,1-F_B)^{\beta}\right\}^{1/\beta}.$$

Another interesting and useful binary operation for implicitly defined point sets is the blend

$$A \mathrm{N} B = \left\{(x,y,z): \left[[F_A(x,y,z)]^{\mathrm{N}} + [F_B(x,y,z)]^{\mathrm{N}}\right]^{\frac{1}{\mathrm{N}}} \geq 0\right\} \tag{13}$$

which has been discussed in this same context by Wyvil et al [32] where the following can be noted:

$$\lim_{\mathrm{N}\to+\infty} A \mathrm{N} B = A \cup B$$

and

$$\lim_{N \to -\infty} A \mathbin{N} B = A \cap B \ .$$

In Figure 4, we show some examples of using these CSG operations. First the head of the female model of Figure 1 is removed ($A - B$) and the stylistic skull of Figure 3 is blended (N = 2.0) on to the body. A "spear" (cylinder plus cone) is unioned in the region of the left abdominal area and then the spear is subtracted ($A - F_{spear}$) from the right stomach area. A zoom-in over the left shoulder serves to show the detail of the blend.

A variety of other interesting operations can be performed on objects that are implicitly defined by volume models by invoking simple operations on the associated field functions. Wyvil et al. [32] have discussed warping operations in the spirit of free form deformations (FFD) [28] and the twist, taper and bend operations of [2] in this context. The whimsical example of Figure 6 shows the results of a taper type of operation where

$$T_{tapir}(x, y, z) = F_{taper} \circ F_{cow}(x, y, z) \ .$$

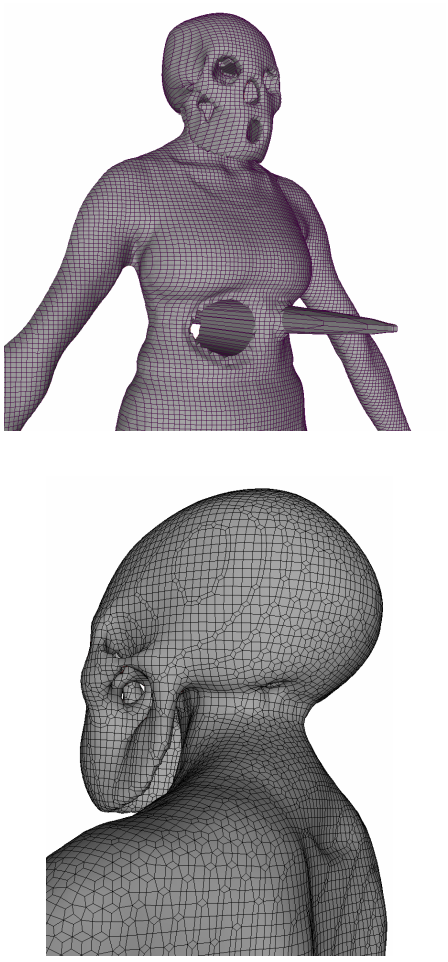

Figure 4. Top image is isosurface from volume model resulting from extended Boolean operation applied to female object of Figure 1 and the skull object of Figure 2. The bottom image gives a view to illustrate the blend of the skull with the female body. Here, we use the MC-Dual surface as described in [22].

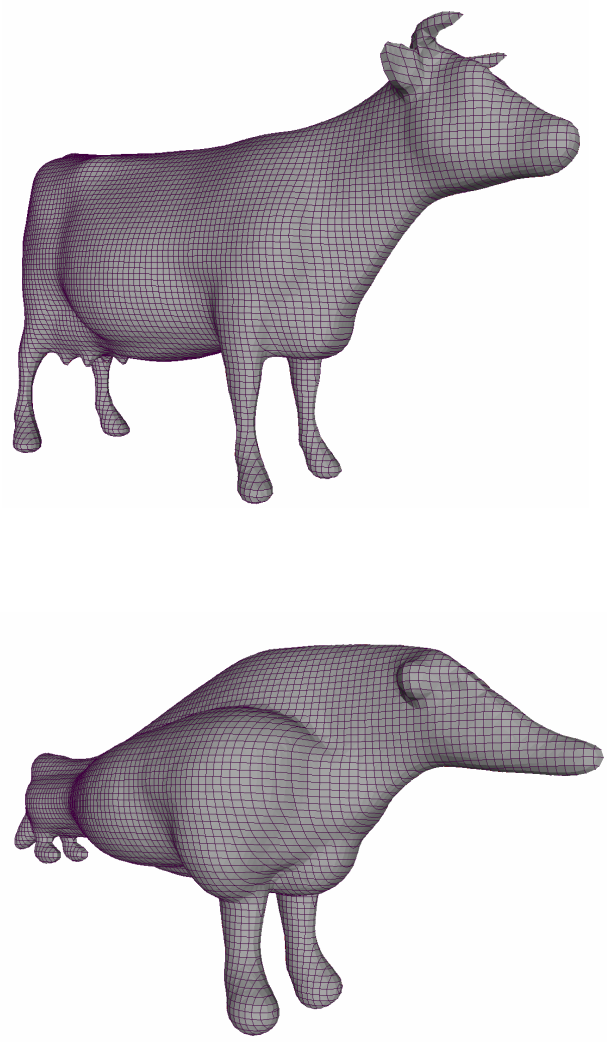

Figure 5. A whimsical example where the top image is an isosurface of a radial Hermite model computed from a polygon surface of a cow from cyberware.com. The bottom image is cow tapered to a tapir!

In the example shown in Figure 6, the radial Hermite interpolant is sampled on a 200x100x200 rectilinear voxel grid and the method of Nielson [21] is used to extract the isosurface. The "pin" was also modeled as an isosurface of a volume model. For this, we simply sampled implicit formulas for cylinders and ellipsoids. We then "subtracted" out the volume of the ball joint to accommodate the "pin" using Boolean operations applied to the respective volume field functions. The image on the left shows the isocontour lines of the voxel grids (4*-network) which also gives a perspective on the resolution of the voxel grid relative to the objects of interest. The images of Figure 7 are two pieces of a mold to be used to make the prosthetic receptacle for the ball. Here we altered the threshold value to accomplish an "offset" to allow some area for lubricants and/or stabilizing material.

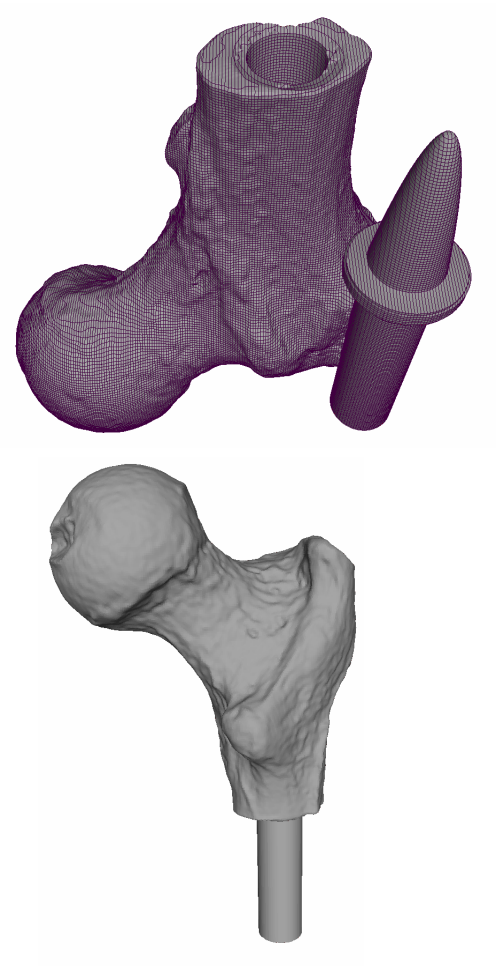

Figure 6. Images of isosurfaces of a volume model which results from Boolean operations applied to implicitly defined objects.

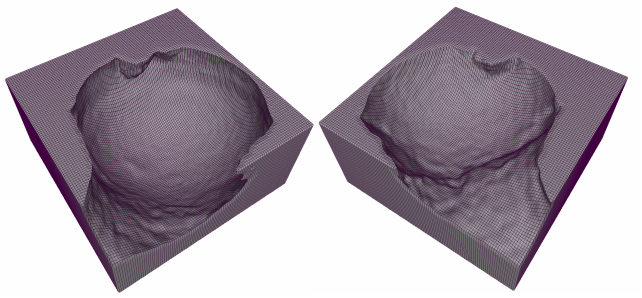

Figure 7. Left and right parts of mold for fabrication of prosthesis for receptacle of ball of the tibia model of Figure 6.

For the example of Figure 8, the field function for a shoe and a foot were sampled over a $240\times160\times120$ lattice. The original triangular mesh for the shoe is from www.fastscan3d.com and consists of 156,474 triangles. The original mesh for the foot model is courtesy of Geomagic and consists of of approximately 20k triangles. The foot is easily subtracted from the shoe using CSG operations.

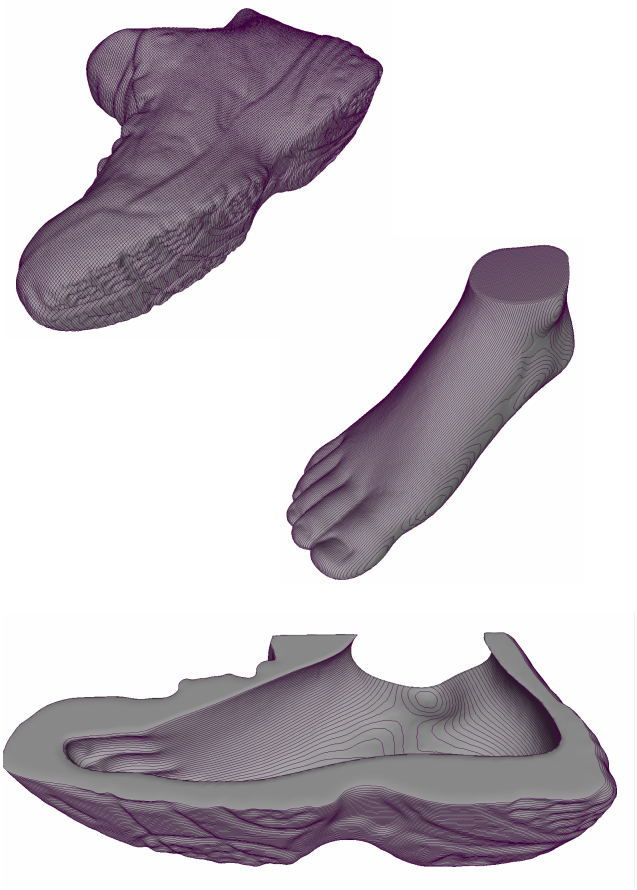

Figure 8. The top images are isosurfaces of a radial Hermite field function defined over a 240x160x120 lattice grid. The bottom model is a cut-away of a Boolean model where the foot has been "subtracted" from the shoe.

4 Mesh Smoothing Examples

In the next two examples we show a very effective method of computing smooth approximations to triangular mesh surface. (See also Bertram [4] and Tasdizen et al. [30].) The idea is extremely simple. Given a polygon mesh surface, we compute a volume model whose zero level, isosurface is an approximation by using the radial Hermite basis functions. Then we apply a 3D weighted average filter to the volume model to produce a "smoothed" volume model from which we recomputed the zero level isosurface which is now a smoothed approximation to the original surface.

In the example of Figure 9 we use a Fourier, high frequency banded filter based upon the "perfect" reconstruction filter $\mathrm{Sin}(x)/x$. The top image of Figure 9 is the isosurface of a $128\times128\times128$ sampling of volume model produced with the radial Hermite operators using $1.5\le\mu_i\le2$ that are based upon the variance of the local point cloud consisting of the closest 24 points. The radius of support, r_i, is the radius of the smallest sphere containing these points. The middle image uses a triple tensor product, reconstruction filter with support on a $9\times9\times9$ voxel region. The support for the bottom image of Figure 9 is a $13\times13\times13$ voxel region.

The example of Figure 10 uses a low resolution model based upon the BLaC wavelets described by Bonneau et al. [5]. These wavelets are a Blend of Linear wavelets and Constant (Haar)

wavelets and we have found them to work rather well in this context. The blend constant for this particular example is 0.43. In this case we compute the tensor product wavelet expansion and then we reconstruct with a certain percentage of the expansion terms with the largest coefficients. The second pair of images of Figure 10 use 95% while the third and fourth pairs of images use 10% and 5% respectively.

Figure 9. The top image is the isosurface of the original volume model. The middle image is from a smoothed volume model using a 9x9x9 filter. The bottom image is based upon a 13x13x13 filter.

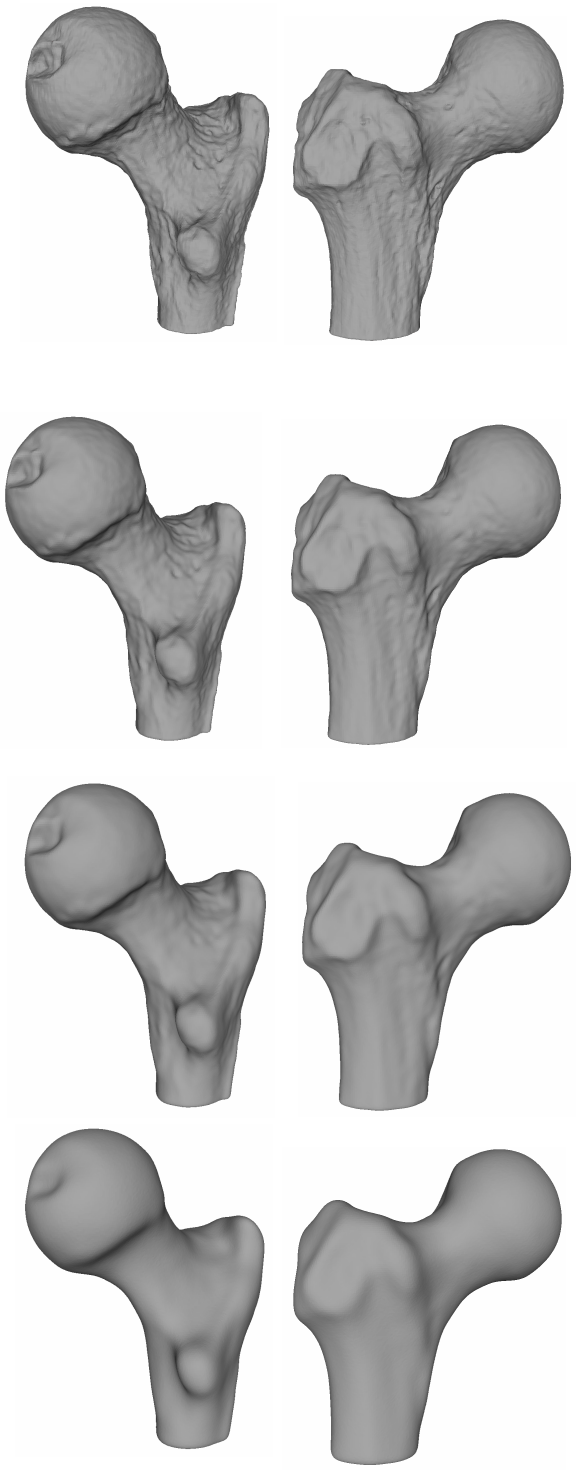

Figure 10. A sequence of isosurfaces from successive application of BLaC wavelet transform applied to the volume model. The top image is the original isosurface and then approximations based upon 95%, 10% and 5% of the largest coefficients of the wavelet expansion.

5 REMARK

The methods that we have described here do not work for noisy data, but incorporating the same models within the context of least squares fitting does lead to efficient and effective methods for noisy data. This will be described in a future report.

Acknowledgments

Thanks to R Holmes, A. Huang, Y. Lu and S. Slyvester for their help. We also wish to acknowledge the support of the Office of Naval Research (N00014-97-1-0243 & N00014-00-1-0281), the National Science Foundation (NSF IIS-9980166 & ACI-0083609) and DARPA (MDA972-00-1-0027).

REFERENCES

[1] J. Algorri and E. Shmitt. Surface reconstruction from unstructured 3D data, *Computer Graphics Forum*, 19:69-81, 2000.

[2] A. Barr. Global and local deformations of solid primitives, *Proceedings of SIGGRAPH 1884*, pages 21-30, ACM Press, 1984.

[3] F. Bernardini, C. Silva, J. Mittleman, H. Rushmeier and G. Taubin. The ball-pivoting algorithm for surface reconstruction, *ACM Transactions on Graphics*, 3:266-286, 1999.

[4] M. Bertram. Fairing scalar fields by vaiational modelling of contours, *Proceedings of Visualization 2003*, pages 387-396, IEEE CS Press, 2003.

[5] G. Bonneau, S. Hahmann and G. M. Nielson. BlaC-Wavelets: A multiresolution analysis with non-nested spaces, *Proceedings of Visualization '96*, pages 43-48. ACM Press, 1996.

[6] J. Carr, R. Beatson, J. Cherrie, T. Mitchell, W, Fright, B. McCallum and T. Evans. Reconstruction and representation of 3D objects with radial basis functions, *Proceedings of SIGGRAPH 2001*, pages 67-76, ACM Press, 2001.

[7] B. Curless and M. Levoy. A volumetric method for building complex models from range images, Proceedings of SIGGRAPH 1996, pages 303-312, ACM Press, 1996.

[8] H. Edelsbrunner and E. Mücke. Three-dimensional alpha shapes, *ACM Transactions on Graphics,* 13:43-72. 1994

[9] M. Floater. Parameterization of trianguations and unorganized points, In *Tutorials on Multiresolution in Geometric Modelling*, I. Aske, E. Quak and M. S. Floater, eds., pages 287-316. Springer, 2002.

[10] R. Franke and G. M. Nielson.. Smooth interpolation to large sets of data, *International Journal Num. Meth. Engn.*, 15:1691-1704. 1980.

[11] R. Franke and G. M. Nielson. Scattered data interpolation and applications: A tutorial and survey, In *Geometric Modelling: Methods and Applications*, H. Hagen & D. Roller, eds., pages 131-160. Springer, 1990.

[12] B. Guo. Surface reconstruction: From points to splines, *CAGD*, 29:269-277, 1997.

[13] I. Hotz. Isometric embedding by surface reconstruction from distances, *Proceedings Visualization 2002*, pages 251-258, IEEE CS Press, 2002.

[14] H. Hoppe, T. DeRose, T. Duchamp, J. McDonald and W. Stuetzle. Surface reconstruction from unorganized points, *Proceedings of SIGGRAPH 1992*, pages 71-78, ACM Press, 1992.

[15] N. Max. Weights for computing vertex normals from facet normals, *Journal of Graphics Tools*, 4:1-6, 1999.

[16] B. Morse, T. Yoo, P. Rheingans, D. Chen and K. Subramanian. Interpolating Implicit Surfaces from Scattered Surface Data Using Compactly Supported Radial Basis Functions. *Proceedings of International Conference on Shape Modeling and Applications '01*, pages 89-98, IEEE CS Press, 2001.

[17] H. Müller. Surface reconstruction – An introduction, In *Scientific Visualization*, H. Hagen, G. Nielson, F. Post, eds., pages 239-242, IEEE CS Press, 1999.

[18] G. M. Nielson. Scattered data modelling, *Computer Graphics and Applications*, 13: 60-7,1, IEEE Press, 1993.

[19] G. M. Nielson. Tools for triangulations and tetrahedrizations, In *Scientific Visualization: Overviews, Methodologies, Techniques*, G. Nielson, H. Hagen & H. Mueller, eds., IEEE CS Press, pages 429-526. 1997.

[20] G. M. Nielson. Volume modeling, In *Volume Graphics*, M. Chen, A. E. Kaufman and R. Yagel, eds., pages 29-48, Springer, 2000.

[21] G. M. Nielson. On marching cubes, *Transactions on Visualization and Computer Graphics*, 9:283-297. 2003

[22] G. M. Nielson. Dual marching cubes, Proceedings of Visualization 2004, this volume, IEEE CS Press, 2004.

[23] G. M. Nielson and J. Tvedt. Comparing methods of interpolation for scattered volumetric data, In *State of the Art in Computer Graphics - Aspects of Visualization*, D. Rogers and R. A. Earnshaw, eds., pages 67-86, Springer, 1994.

[24] G. M. Nielson and A. Huang. Approximating normals for marching cubes applied to locally supported isosurfaces, *Proceedings of Visualization 2002*, pages 459-466. IEEE CS Press, 2002.

[25] G. M. Nielson, H. Hagen and K. Lee. Split 'N Fit: Adaptive least squares fitting of triangular mesh surfaces to scattered point cloud data, In *Scientific Data Visualization*, Bonneau, Ertl & Nielson, eds., pages 19-43, Springer, 2004.

[26] V. Savchenko, A. Pasko, O. Okunev and T. Kunii. Function representation of solids reconstructed from scattered surface points and contours, *Computer Graphics Forum*, 14:181-188. 1995.

[27] L. Schumaker. Scattered data approximation, In *Approximation Theory II*, pages 123-145. Academic Press, 1976.

[28] T. Sederberg and S. Parry. Free-from deformations of solid geometric models, *Proceedings of SIGGRAPH 1986*, pages 151-160. ACM Press, 1986.

[29] C. Sigg, R. Peikert and M. Gross. Signed distance transformation using graphics hardware, *Proceedings of Visualization 2003*, pages 83-90. IEEE CS Press, 2003.

[30] T. Tasdizen, R. Whitaker, Burchard and S. Osher. Geometric surface smoothing via ansistropic diffusion of normals, *Proceedings of Visualization 2002*, pages 125-132. IEEE CS Press, 2002.

[31] G. Turk and J. O'Brien. Shape transformation using variational implicit functions, *Proceedings of SIGGRAPH 1999*, pages 335-342, ACM Press, 1991.

[32] B. Wyvill, A. Guy and E. Galin. Extending the CSG tree warping, blending and Boolean operations in an implicit surface modelling system, *Proceedings of Implicit Surfaces* 1998. pages 123-456. IEEE CS Press, 1998.

[33] H. Xie, J. Wang, J. Hua, J. Qin, A. Kaufman. Piecewise C1 continuous surface reconstruction of noisy point clouds via local implicit quadric regression, *Proceedings of IEEE Visualization 2003*, pages 91-98. IEEE CS Press, 2003.

[34] H. Zhao, S. Osher and F. Fedkiw. Fast surface reconstruction using the level set method, *Proceedings 8th International Conference on Computer Vision (ICCV)*, Vancouver, Canada, pages 194-202. IEEE Press, 2001.